ADVANCED MATERIALS

[10] W. Zhang, S. Y. Chou, *Appl. Phys. Lett.* **2003**, *83*, 1632.
[11] Y. Chen, D. Macintyre, E. Boyd, D. Moran, I. Thayne, S. Thoms, *J. Vac. Sci. Technol. B* **2002**, *20*, 2887.
[12] D. Pisignano, L. Persano, P. Visconti, R. Cingolani, G. Gigli, G. Barbarella, L. Favaretto, *Appl. Phys. Lett.* **2003**, *83*, 2545.
[13] X. Cheng, Y. T. Hong, J. Kanicki, L. J. Guo, *J. Vac. Sci. Technol. B* **2002**, *20*, 2877.
[14] Y. Hirai, S. Harada, H. Kikuta, Y. Tanaka, M. Okano, S. Isaka, M. Kobayasi, *J. Vac. Sci. Technol. B* **2002**, *20*, 2867.
[15] J. Wang, S. Schablitsky, Z. N. Yu, W. Wu, S. Y. Chou, *J. Vac. Sci. Technol. B* **1999**, *17*, 2957.
[16] J. Wang, X. Y. Sun, L. Chen, S. Y. Chou, *Appl. Phys. Lett.* **1999**, *75*, 2767.
[17] L. J. Guo, X. Cheng, C. Y. Chao, *J. Mod. Opt.* **2002**, *49*, 663.
[18] W. Wu, B. Cui, X. Y. Sun, W. Zhang, L. Zhuang, L. S. Kong, S. Y. Chou, *J. Vac. Sci. Technol. B* **1998**, *16*, 3825.
[19] G. M. McClelland, M. W. Hart, C. T. Rettner, M. E. Best, K. R. Carter, B. D. Terris, *Appl. Phys. Lett.* **2002**, *81*, 1483.
[20] H. Cao, Z. N. Yu, J. Wang, J. O. Tegenfeldt, R. H. Austin, E. Chen, W. Wu, S. Y. Chou, *Appl. Phys. Lett.* **2002**, *81*, 174.
[21] L. J. Guo, X. Cheng, C. F. Chou, *Nano Lett.* **2004**, *4*, 69.
[22] A. Pepin, P. Youinou, V. Studer, A. Lebib, Y. Chen, *Microelectron. Eng.* **2002**, *61*, 927.
[23] J. D. Hoff, L. J. Cheng, E. Meyhofer, L. J. Guo, A. J. Hunt, *Nano Lett.* **2004**, *4*, 953.
[24] *Technol. Rev.* **2003**, *106*, 36.
[25] G. Y. Jung, S. Ganapathiappan, X. Li, D. A. A. Ohlberg, D. L. Olynick, Y. Chen, W. M. Tong, R. S. Williams, *Appl. Phys. A.* **2004**, *78*, 1169.
[26] D.-Y. Khang, H. H. Lee, *Appl. Phys. Lett.* **2000**, *76*, 870.
[27] M. Colburn, I. Suez, B. J. Choi, M. Meissl, T. Bailey, S. V. Sreenivasan, J. G. Ekerdt, C. G. Willson, *J. Vac. Sci. Technol. B* **2001**, *19*, 2685.
[28] J. V. Crivello, *Polym. Eng. Sci.* **1992**, *32*, 1462.
[29] R. Xie, A. Karim, J. F. Douglas, C. C. Han, R. A. Weiss, *Phys. Rev. Lett.* **1998**, *81*, 1251.
[30] U. Thiele, M. G. Velarde, K. Neuffer, *Phys. Rev. Lett.* **2001**, *87*, 016 104.
[31] S. Herminghaus, K. Jacobs, K. Mecke, J. O. R. Bischof, A. Fery, M. Ibn-Elhaj, S. Schlagowski, *Science* **1998**, *282*, 916.
[32] H. I. Kim, C. M. Mate, K. A. Hannibal, S. S. Perry, *Phys. Rev. Lett.* **1999**, *82*, 3496.
[33] R. Yerushalmi-Rozen, J. Klein, *Langmuir* **1995**, *11*, 2806.
[34] W. D. Harkins, *The Physical Chemistry of Surface Films*, Reinhold, New York **1952**, p. 175.
[35] G. L. Gaines, Jr., *Macromolecules* **1981**, *14*, 208.
[36] F. Garbassi, M. Morra, E. Occhiello, *Polymer Surfaces from Physics to Technology*, Wiley, New York **1994**, p. 301.
[37] J. V. Crivello, J. L. Lee, *J. Polym. Sci., Part A: Polym. Chem.* **1990**, *28*, 479.

Size Distribution of Cobalt Nanocrystals: A Key Parameter in Formation of Columns and Labyrinths in Mesoscopic Structures**

By *Vincent Germain* and *Marie-Paule Pileni**

In the last decade, several studies have been undertaken to ascertain the patterns induced by applying a magnetic field perpendicular to the plane of mesoscopic films.[1] These patterns evolve from disordered to ordered dots and then to labyrinthine structures.[2,3] In most cases, these magnetic-field effects are observed at rather low fields corresponding to the zone of linear response to the applied magnetic field. Similar patterns were obtained by applying a rather high magnetic field during the evaporation of a fluid containing cobalt nanocrystals dispersed in a non-polar solvent.[4] However, a thick film of cobalt nanocrystals underneath such "supra" structures was observed. In these cases the applied magnetic fields, in addition to being rather high, were located in the region of nonlinear response. Furthermore, the nanocrystals dispersed in the non-magnetic fluid had a fairly wide size distribution. Very recently we succeeded in producing cobalt nanocrystals with a very narrow size distribution, making it possible to form either two-dimensional monolayers in compact hexagonal networks or three-dimensional "supra" crystals in face-centered cubic (fcc) structures.[5]

Here, we demonstrate that the size distribution of magnetic cobalt nanocrystals is the key parameter in controlling the morphology of the mesoscopic patterns, i.e., controlling the formation of columns or labyrinthine structures.

The synthesis of cobalt nanocrystals with a low size distribution has been described previously.[6] Reverse micelles of 5×10^{-2} M cobalt di(ethylhexyl)sulfosuccinate, usually called $Co(AOT)_2$,[7] with a water content $w = [H_2O]/[AOT] = 32$, were formed in a $Co(AOT)_2$/isooctane/water system. $Co(AOT)_2$ was reduced by sodium borohydride, $NaBH_4$, and its amount was determined by monitoring the ratio, $R = [NaBH_4]/[Co(AOT)_2]$. The nanocrystals were coated by adding lauric acid ($C_{12}H_{25}COOH$), which induced covalent attachment with cobalt atoms located at the interface.[8] The coated cobalt nanocrystals were then extracted from the solution by addition of ethanol. These nanocrystals were washed and centrifuged several times with ethanol to remove all the surfactant molecules and then dispersed in hexane, in which the cobalt nanocrystal concentration was set to 4.8×10^{-4} mol L^{-1}. Cobalt acetate, lauric acid, and sodium borohydride were obtained from

[*] Prof. M.-P. Pileni, Dr. V. Germain
Laboratoire LM2N, Université P. et M. Curie (Paris VI)
B.P. 52, 4 Place Jussieu, F-75231 Paris Cedex 05 (France)
E-mail: pileni@sri.jussieu.fr

[**] We are grateful to Dr. D. Ingert and Dr. J. Richardi for many fruitful discussions.

  DOI: 10.1002/adma.200401559

Aldrich; isooctane and hexane were obtained from Fluka; di(ethylhexyl)sulfosuccinate was obtained from Sigma. All the chemicals were used without further purification.

Control of the size of the nanocrystals and their distribution was obtained by two different methods:

i) As already demonstrated, the syntheses, which were carried out at various R values, induced formation of nanocrystals with different size distributions and slight variations in average size.[6]

ii) The products of several syntheses under the same experimental conditions were mixed together, inducing an increase in the size distribution.

For any procedure, the magnetic properties of the nanocrystals of a given average size remained quite similar, with an unchanged saturation magnetization.

The mesostructures were produced as previously described:[4] the magnetic fluid (200 μL) was deposited in a beaker containing a copper transmission electron microscopy (TEM) grid covered with amorphous carbon, which was used as the substrate. The beaker was then covered with parafilm to lower the evaporation rate and was subjected (or not) to an external magnetic field (0.25 T) perpendicular to the substrate. The solvent was slowly evaporated and the magnetic field was applied until evaporation was complete. At the end of the evaporation, the copper TEM grid was removed and the mesoscopic structures were observed using TEM[9] and scanning electron microscopy (SEM).[10] In some cases, a highly oriented pyrolitic graphite (HOPG) substrate instead of a TEM grid was used; these specific cases will be noted in the text. The magnetic field was produced either by a permanent magnet[11] or an electromagnet;[12] the mesostructures were not affected by the type of magnet used. Furthermore, the SEM patterns remained similar for various concentrations of cobalt nanocrystals (from 2×10^{-4} to 9.5×10^{-3} M). The initial cobalt concentration was kept at 4.76×10^{-4} mol L^{-1}.

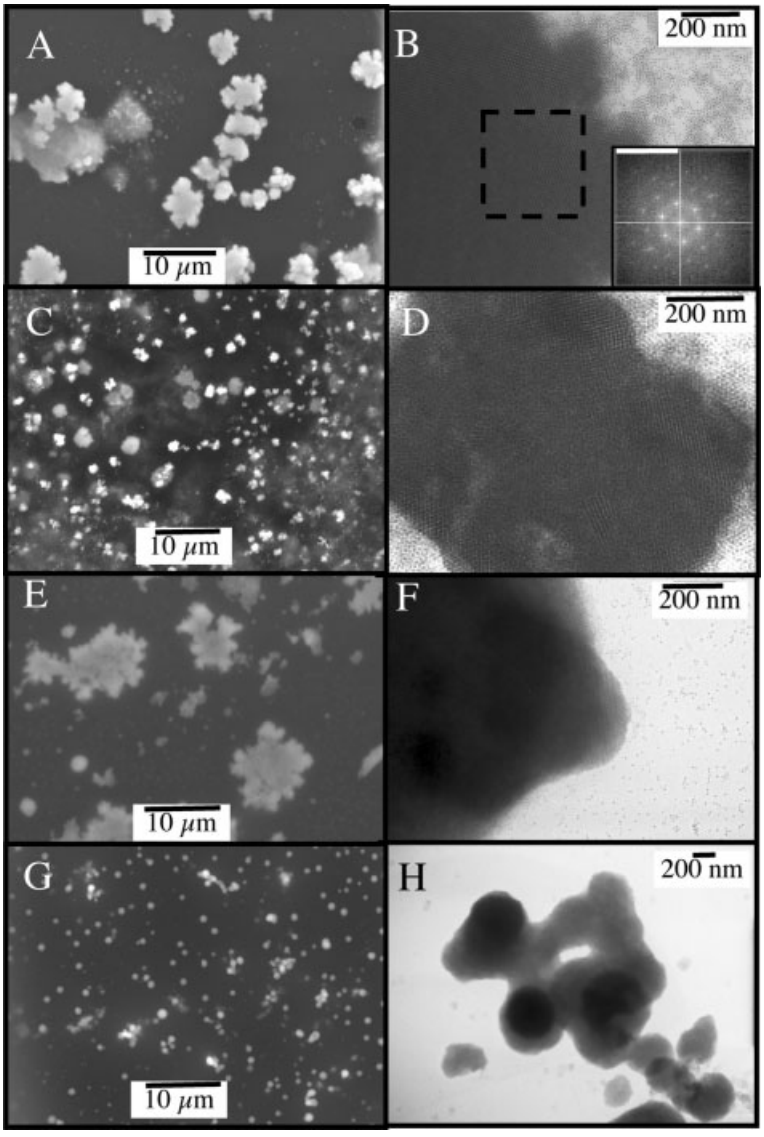

Figure 1. SEM (A, C, E, G) and TEM (B, D, F, H) images of aggregates made of cobalt nanocrystals with different sizes: 5.7 nm (A, B), 7.1 nm (C, D), 8.1 nm (E, F), 6.9 nm (G, H), and different size distributions: 13 % (A, B), 11.4 % (C, D), 10.3 % (E, F), 18 % (G, H). No magnetic field was applied. Inset in B: FFT of the area delimited by the dashed line, the scale bar represents 86 nm^{-1}.

In the following, we consider the mesostructures obtained in the absence and presence of an applied magnetic field with cobalt nanocrystals of different average sizes and distributions. The mesostructures were observed at low magnification by SEM, whereas TEM was used to record images at high magnification.

Let us first consider nanocrystals of various average sizes with low size distributions. In the absence of an applied magnetic field, nanocrystals with an average diameter, $D = 5.7$ nm and size distribution, $\sigma_D = 13$ % produced large aggregates with sizes between 2.5 and 9 μm (Fig. 1A). On magnifying the image of these aggregates, well-defined superlattices of nanocrystals (Fig. 1B) were observed. The fast Fourier transform (FFT) of a given area of the superlattice (Fig. 1B, inset) exhibits sixfold symmetry, indicating ordering of the nanocrystals in an fcc structure. This agrees with previous results, in which "supra" crystals in fcc structures were produced.[5] On increasing the average size of the nanocrystals to 7.1 nm and keeping a low size distribution ($\sigma_D = 11.4$ %), similar behavior was obtained with the formation of large aggregates (Fig. 1C) and the observation of well-defined nanocrystal ordering at higher magnification (Fig. 1D). Figures 1E,F confirm this same behavior for nanocrystals for which $D = 8.1$ nm, and $\sigma_D = 10.3$ %. These data clearly indicate formation of large aggregates ordered in an fcc structure when cobalt nanocrystals with a low size distribution (≤13 %) are deposited in the absence of a magnetic field (Table 1) and do not depend on the average nanocrystal size in the 5 to 8 nm range.

ADVANCED MATERIALS

Table 1. Influence of the cobalt nanocrystal size with various size distributions on the patterns obtained in the absence of a 0.25 T applied magnetic field. $\sum_D$: distribution of the nanoparticle diameters expressed in nm; D_A: size of the aggregates, assuming they are spherical; H_A: height of the aggregates; σ_{HA}: height distribution in percentage; W_A: width of the aggregates; σ_{WA}: width distribution in percentage; *AR*: aspect ratios of the columns.

D [nm]	5.7	7.1	8.1
σ_D [%]	13	11.4	10.3
Σ_D [nm]	0.74	0.81	0.84
D_A [μm]	2.5–9	1.3–6	1.8–6
Mesostructures	columns	columns	columns
H_A [μm]	5	5.2	3.5
σ_{HA} [%]	12	11.5	17.1
W_A [μm]	1.7 (0.85)	0.84	0.66
σ_{WA} [%]	19.4	17.9	18.2
AR	5.9	6.2	5.3

When a magnetic field (0.25 T) was applied during the evaporation process, the mesostructures, produced with the same nanocrystals as those described above, markedly differed (Fig. 2). For nanocrystals of average diameter 5.7 nm with $\sigma_D = 13$ %, well-defined cylinders with a rather low size distribution were observed (Fig. 2A). From video observation,[13] we know that straight columns were formed in solution during the evaporation. At the end of this process they fell on the substrate because of capillary forces, and appeared as cylinders. In the following, we call them columns. Figure 2B shows that their extremities were made of well-ordered nanocrystals; an FFT was performed on the area demarcated by the dashed line. The FFT pattern (Fig. 2B, inset) has fourfold symmetry, as expected for fcc crystals in the [100] direction. Due to the thickness of the patterns, it was impossible to observe the ordering inside the columns by TEM, and the lack of material prevented any small-angle X-ray spectroscopy (SAXS) measurements. From data already obtained on "supra" crystals and from Figure 2B, it is concluded that the columns were made of nanocrystals ordered in an fcc structure. Similar data, with well-ordered columns, were obtained with nanocrystals of average diameter 7.1 nm with a 11.4 % size distribution (Fig. 2C). In some TEM images, a "foot" of the columns remained stacked on the substrate, as shown in Figure 2D. This remaining "foot" and the end of the fallen column were found to consist largely of well-ordered nanocrystals. This was confirmed by the FFT (Fig. 2D, inset), which shows sixfold symmetry, as expected for fcc crystals in the [111] direction. This pattern is not as well-defined as that seen in the inset of Figure 1A because the observed area corresponding to the "foot" of the column was rather rough and induced a lattice mismatch. As for smaller nanocrystals, it is reasonable to conclude that the nanocrystals forming the columns were ordered in an fcc structure. Similar behavior was obtained for nanocrystals of average size 8.1 nm with $\sigma = 10.3$ % (Figs. 2E,F). Except for the sample shown in Figure 2A, for any nanocrystal diameter (in the 5.5 to 8 nm range) the average aspect ratio of the column remained unchanged. This apparent discrepancy, observed in Figure 2A ($D = 5.7$ nm, $\sigma_D = 13$ %), is related to second-level hexagonal patterns. These patterns depend on the real-time phase transition in the structure formation observed by Hong et al.[14] with a magnetic fluid in a Hele–Shaw cell. In fact, each observed entity consists of two columns (Fig. 2A, inset). By changing the evaporation rate and/or lowering the diffusion of the nanocrystals, well-defined columns were produced (see below). It can then be concluded that each column observed in Figure 2A is, in fact, made of two entities with an average height and width of 5 μm and 0.85 μm, respectively. Taking into account formation of these two columns close to each other, the aspect ratios of columns made of nanocrystals of different diameters (from 5.5 to 8 nm) with low size distributions are of the same order of magnitude (Table 1). Furthermore, mesostructure patterns of cobalt nanocrystals of different sizes with low size distributions are made of columns ordered in fcc structures.

No transition from columns to labyrinths took place on increasing the strength of the applied magnetic field. Figures 3A–C show SEM patterns of cobalt nanocrystals (for which $D = 7.1$ nm and $\sigma = 11.4$ %) that were subjected to various magnetic field strengths (0.25 T, 0.46 T, and 0.59 T, respectively) during deposition. For any given magnetic field strength, columns of the same average height and width were produced (Table 2). From these data, it is concluded that the same patterns are produced at various strengths of the applied field (from 0.25 to 0.59 T). Table 2 shows that the average length, width, and aspect ratio remained within the same order of magnitude on increasing the strength of the applied field. This is because the applied magnetic field strength is rather high and corresponds to the zone where the magnetic response of the nanocrystals is close to saturation (i.e., the nonlinear regime). These data obtained at various applied magnetic field strengths disagree with those obtained in our laboratory using cobalt nanocrystals of diameter 8 nm with a 14 % size distribution:[4] transition from disordered to ordered columns, followed by formation of labyrinths and/or worm-like structures was observed. Furthermore, the column heights markedly decreased on increasing the applied field strength. The major differences between the present and published data are the size distributions. Let us then consider cobalt nanocrystals that have the same average diameter (around 6 nm) but which have different size distributions. The substrate (HOPG) is chosen to be the same as that used in previous work[4] and the applied field strength is 0.25 T. The major difference between the substrate used above (TEM grid covered by an amorphous layer of carbon) and HOPG is that the TEM grid is rough. In fact, the copper TEM substrate is made of a grid, creating "holes" which prevent the nanocrystals from diffusing freely on the surface. "Fallen" and upright

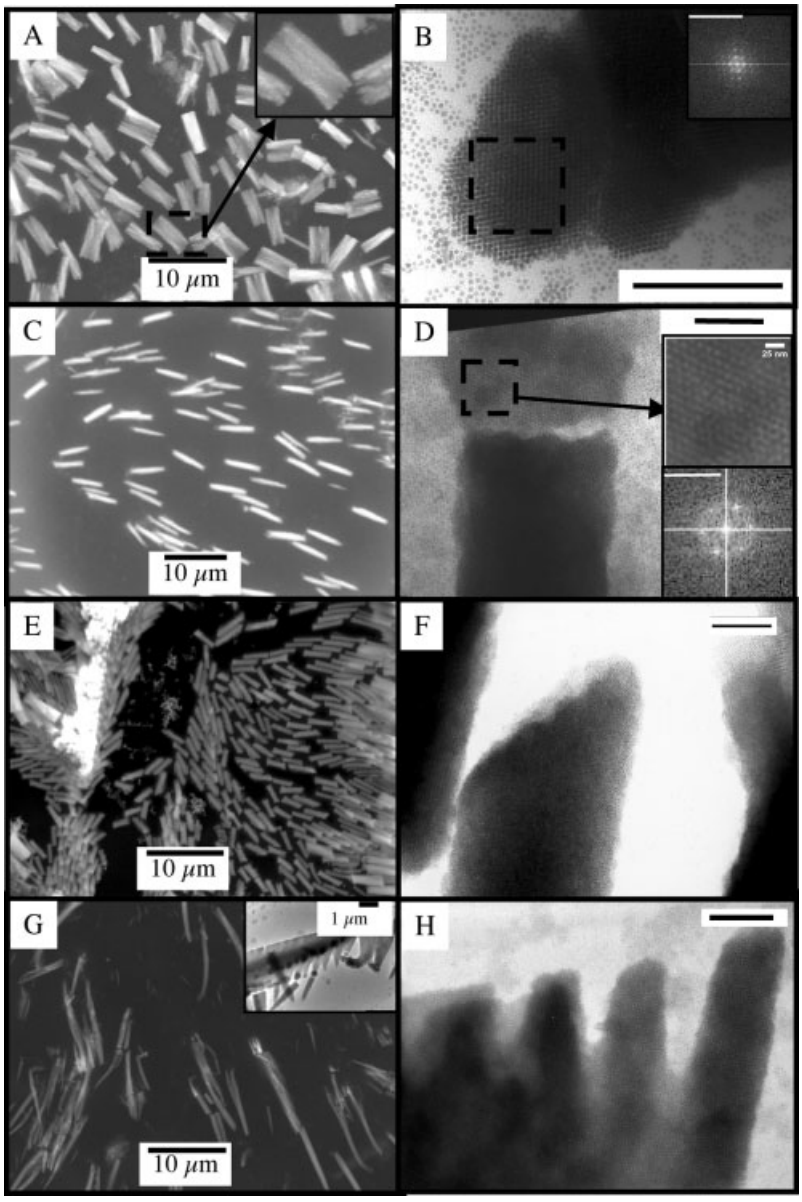

Figure 2. SEM (A, C, E, G) and TEM (B, D, F, H) images of mesostructures made of cobalt nanocrystals with different sizes: 5.7 nm (A, B), 7.1 nm (C, D), 8.1 nm (E, F), 6.9 nm (G, H), and different size distributions: 13 % (A, B), 11.4 % (C, D), 10.3 % (E, F), 18 % (G, H) subjected to a 0.25 T magnetic field applied perpendicularly to the substrate. For B, D, F, and H the scale bars represent 200 nm. Inset in A: Magnified view of a column. Inset in B: FFT of the area delimited by the dashed line, the scale bar represents 58.26 nm^{-1}. Inset in D: Magnified view of the TEM image and FFT of the magnified area, the scale bar in the FFT pattern represents 20.96 nm^{-1}.

columns, containing nanocrystals of average diameter 5.7 nm and size distribution 13 %, and with well-defined heights (3.05 μm ± 9 %) and widths (1.7 μm ± 7 %) were formed, as shown in Figure 3E. On increasing the size distribution of the nanocrystals from 13 to 16.8 % with an average particle diameter of 5.9 nm, longer columns formed, which were either isolated on the substrate or associated with each other, as shown in Figure 3F. The number of isolated columns markedly decreased compared to that obtained using nanocrystals of lower size distribution, average height (1.36 μm ± 7.5 %), and width (0.2 μm ± 16 %). Magnification of the pattern (Fig. 3F, left inset) shows that the columns were aligned and tended to fuse together to form a worm-like structure. In some parts of the SEM images, large aggregates are observed and are attributed to a change in the orientation of the fused columns (Fig. 3F, right inset). A further increase in the size distribution (18 %) with the same average nanocrystal diameter (5.9 nm) induced formation of longer columns (3.8 μm and 0.7 μm in height and width, respectively). A further decrease in the isolated columns was observed, whereas the number of aggregates formed by fusion of columns with similar sizes increased. The number of columns was not large enough to give a size distribution. This aggregation explains, on a larger scale, the appearance of worm-like and labyrinth structures (see arrows in the inset of Fig. 3G). The pattern obtained with cobalt nanocrystals of average diameter 7 nm and size distribution 20 % shows simultaneous formation of labyrinths and columns (Fig. 3H). A highly magnified view of these labyrinths shows that they are made of coalesced cylinders (Fig. 3H, right inset). In fact, when the size distribution was large, columns of various lengths and widths were formed. Because the columns were formed in solution, the entities of similar sizes tended to self-assemble via van der Waals' interactions. The large dispersion in nanocrystal size induced some defects at the border of the columns, thus favoring their coalescence. The large dispersion in the height of the columns induced the formation of labyrinths of various heights. This is clearly seen in the left inset of Figure 3H. Because the nanocrystals diffused freely during evaporation, some size segregation took place, inducing the formation of well-defined columns. This explains why some columns were produced and their number decreased on increasing the size distribution. From this, it is concluded that the size distribution of nanocrystals is the key parameter that determines the formation of columns, worm-like structures, or labyrinths. The latter are produced by agglomeration of cylinders that have, more or less, the same size.

To understand the growth of the columns and the influence of the nanocrystal size distribution on the patterns, let us first consider the mesoscopic structure obtained in the absence of an applied magnetic field with nanocrystals of average diameter 6.9 nm and a rather large size distribution ($\sigma_D = 18$ %). Fig-

ADVANCED MATERIALS

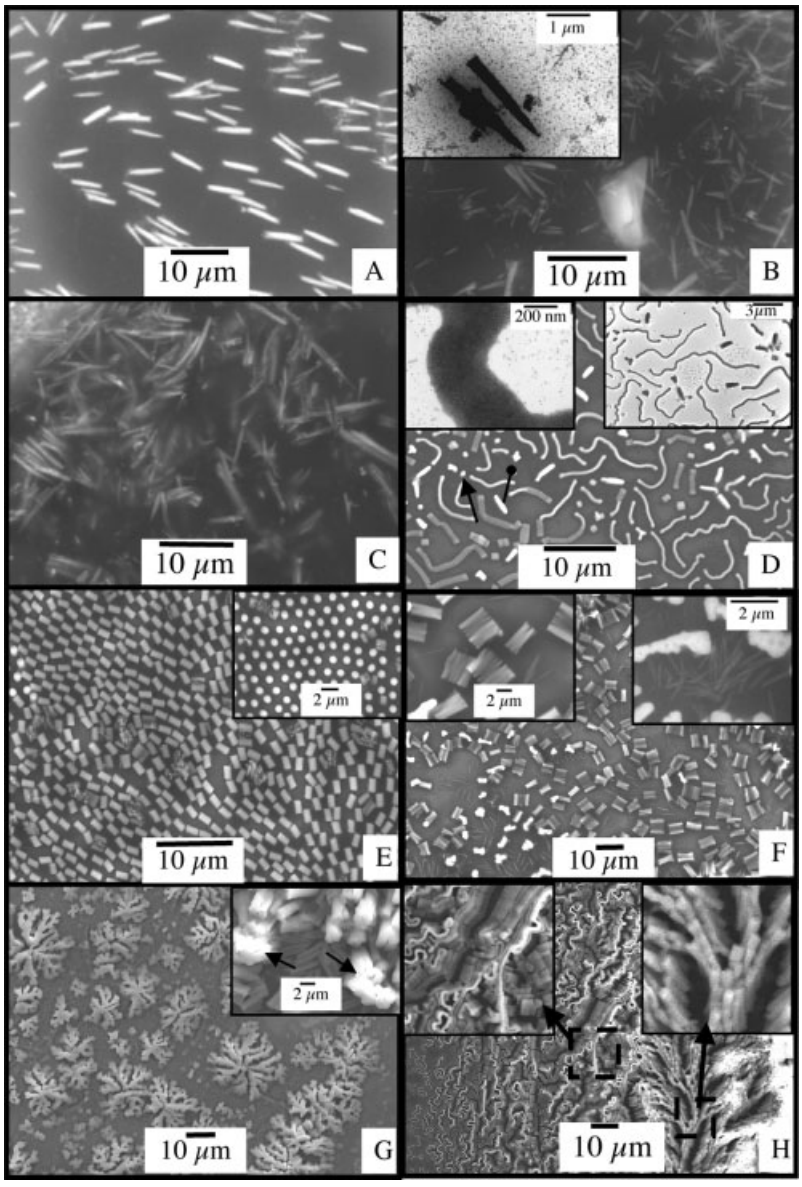

Figure 3. A–C) SEM images of mesostructures of cobalt nanocrystals ($D = 7.1$ nm, $\sigma_D = 11.4\,\%$) obtained by applying a perpendicular magnetic field of varying strength: 0.25 T (A), 0.46 T (B), and 0.59 T (C). Inset in B: TEM pattern of columns. D: SEM mesostructure obtained with cobalt nanocrystals ($D = 8.7$ nm, $\sigma_D = 20\,\%$); left inset: TEM image of the same sample. right inset: enhancement of the TEM image. E–H) SEM images of mesostructures of nanocrystals with different size distributions obtained on applying a 0.25 T perpendicular magnetic field; E: ($D = 5.7$ nm, $\sigma_D = 13\,\%$), F: ($D = 5.9$ nm, $\sigma_D = 16.8\,\%$), G ($D = 5.9$ nm, $\sigma_D = 18\,\%$), and H ($D = 8.7$ nm, $\sigma_D = 20\,\%$).

ure 1G shows that the size of the aggregates markedly drops (between 0.4 and 1.6 μm) compared to those of aggregates produced from nanocrystals that had a similar average diameter and a lower size distribution (between 2.5 and 9 μm). Furthermore, a magnified view of these aggregates shows that the nanocrystals were randomly deposited (Fig. 1H), whereas they were arranged in fcc structures for a low distribution. As expected,[15] the nanocrystal ordering in these fcc structures markedly depends on the size distribution. Note that the aggregates shown in Figure 2H are not compact. When the nanocrystals were subjected to a 0.25 T applied magnetic field at the end of the evaporation process, the columns were no longer well-defined (Fig. 2G) and had a rather large disorder. In addition, at the ends of the columns and along the columns, "finger"-like patterns appeared (Fig. 2G, inset; Fig. 2H). This is related to the fact that small aggregates without any ordered structure are observed when these nanocrystals were not subjected to an applied magnetic field (Figs. 1E,F). The formation of columns with many defects is explained as follows: when the liquid–gas transition takes place, the columns start to grow on rough and deformed aggregates. This disorder induces defects during column growth and results in the patterns observed in Figures 2E,F. Hence, a large change in the mesoscopic patterns with the size distribution of the nanocrystals used to make the mesoscopic structures is observed. To confirm this claim, the mesoscopic pattern produced in a 0.25 T applied magnetic field is made of cobalt nanocrystals (8.7 nm) with a rather large size distribution (20 %). Figure 3D shows, by SEM, formation of labyrinths on a large scale. Some are very long and others are worm-like; the arrows point to columns and the fusion of two columns. A similar pattern is observed by TEM (Fig. 3D, inset). Magnification of the TEM image shows that the labyrinths were formed with disordered nanocrystals (Fig. 3D, inset).

From these results and considerations, it is claimed that applying a magnetic field perpendicular to the substrate during evaporation produces well-defined columns of cobalt nanocrystals with a low size distribution. The size of the columns depends neither on the nanocrystal diameters in a 5.5 to 8 nm range nor on the applied field strength. The key parameter in column formation is the nanocrystal size distribution. At low size distributions, the nanocrystals self-assemble into fcc structures; they are closely packed. This induces strong cohesion inside columns with the same height, width, and aspect ratio for any applied field strength. The increase in the nanocrystal distribution destroys the cohesion because the system is unable to form a compact structure, and disordered aggregates are produced. This creates defects at the ends of the columns and at their edges, favoring their fusion in labyrinths. From this, it is concluded that labyrinths are a product of the fusion of columns. This agrees with calculations

Table 2. Influence of the applied magnetic field strength on the patterns obtained with cobalt nanocrystals of average diameter 7.1 nm and 11.4 % size distribution.

Applied magnetic field [T]	0.25	0.46	0.59
H_A [μm]	5.2	4	5.3
σ_{HA} [%]	11.5	16.25	20.8
W_A [μm]	0.84	0.62	0.7
σ_{WA} [%]	17.9	24.2	25.7
AR	6.2	6.15	7.5

made in our laboratory[16] and by other groups,[3] which show that, energy being the same, columns and labyrinths are produced.

Received: September 22, 2004
Final version: March 3, 2005

[1] M. D. Cowley, R. E. Rosensweig, *J. Fluid Mech.* **1997**, *30*, 671.
[2] C. Y. Hong, I. J. Jang, H. E. Horng, C. J. Hsu, Y. D. Yao, H. C. Yang, *J. Magn. Magn. Mater.* **1999**, *201*, 317.
[3] A. L. Dickstein, S. Erramilli, R. E. Goldstein, D. P. Jackson, S. A. Langer, *Science* **1993**, *261*, 1012.
[4] J. Legrand, A. T. Ngo, C. Petit, M. P. Pileni, *Adv. Mater.* **2001**, *13*, 58.
[5] I. Lisiecki, P. A. Albouy, M. P. Pileni, *Adv. Mater.* **2003**. *15*, 712.
[6] I. Lisiecki, M. P. Pileni, *Langmuir* **2003**, *19*, 9486.
[7] C. Petit, P. Lixon, M. P. Pileni, *J. Phys. Chem.* **1990**, *94*, 1598.
[8] N. Wu, L. Fu, M. Su, M. Aslam, K. C. Wong, V. P. Dravid, *Nano Lett.* **2004**, *4*, 383.
[9] TEM micrographs were obtained using a JEOL 100 CXII at 100 kV.
[10] SEM was done with a JMS-5510LV instrument.
[11] The field intensity measured with a magnetometer was 0.25 T.
[12] Magnet power supply: Oxford Instruments PS2-120. Electromagnet: Oxford Instruments N38. The intensity of the magnetic field was variable. We chose 0.46 T and 0.59 T for the experiments.
[13] V. Germain, M. P. Pileni, unpublished.
[14] C. Y. Hong, H. E Horng, S. Y. Yang, H. C. Yang, J. M. Wu, *Appl. Phys. Lett.* **1999**, *75*, 2196.
[15] M. P. Pileni, *J. Phys. Chem. B.* **2001**, *105*, 3358.
[16] J. Richardi, M. P. Pileni, *Phys. Rev. E* **2004**, *69*, 016 304.

Super-Stable, High-Quality Fe_3O_4 Dendron–Nanocrystals Dispersible in Both Organic and Aqueous Solutions**

By *Myeongseob Kim*, *Yongfen Chen*, *Yongcheng Liu*, and *Xiaogang Peng**

High-quality Fe_3O_4 nanocrystals and other magnetic oxide nanocrystals with desirable surface coatings are attractive nanomaterials for fundamental studies[1–3] and technical applications such as in magnetic fluids,[4] drug delivery,[5,6] magnetic resonance imaging, sensing,[7,8] and data storage and processing.[9] These purposes require the nanocrystals to be dispersible and stable in a variety of media. High-quality magnetic oxide nanocrystals—nearly monodisperse in size and shape, highly crystalline, and available in a large size range—have recently become available through several relatively simple synthetic strategies.[10–13] Surface modification of these high-quality magnetic oxide nanocrystals is an essential and challenging step for most of their technical applications and fundamental studies, because the as-synthesized nanocrystals are only soluble in non-polar solvents and not sufficiently stable for necessary manipulations. In this communication, we introduce a new class of ligands, poly(ethylene glycol) (PEG)-terminated organic dendrons with a hydroxamic acid group (a known strong-bonding group for bulk iron oxide surfaces)[14] located at the focal point (Fig. 1, top left), for stabilizing magnetic oxide nanocrystals, thus producing so-called dendron–nanocrystals.

The multiple PEG-oligomer terminal groups of the dendron ligands were designed for versatile dispersion of the resulting nanocrystals. Different from the dendron ligands used for semiconductor and noble-metal nanocrystals,[15–17] the terminal generation of the dendrons was designed to be asymmetric (Fig. 1). The double bond provides a potential crosslinking or conjugating site for chemical and biochemical functional species.

The high-quality Fe_3O_4 nanocrystals (Fig. 2, bottom right) used in this work were synthesized via a recently published procedure using stearic acid as the ligands.[13] The as-prepared nanocrystals were soluble in typical non-polar solvents, but were not very stable against moderate chemical treatments. For instance, these nanocrystals could hardly survive more than two precipitations from their solvents. The ligand exchange

[*] Prof. X. Peng, Dr. M. Kim, Dr. Y. Chen
Department of Chemistry and Biochemistry
University of Arkansas
Fayetteville, AR 72701 (USA)
E-mail: xpeng@uark.edu
Dr. Y. Liu
NN-Labs, LLC
Fayetteville, AR 72701 (USA)

[**] Supporting Information is available online from Wiley InterScience or from the author.

 DOI: 10.1002/adma.200401991